NOAA Technical Report ERL 329-WPL 39

U.S. DEPARTMENT OF COMMERCE
NATIONAL OCEANIC AND ATMOSPHERIC ADMINISTRATION
Environmental Research Laboratories

FM-CW Boundary Layer Radar With Doppler Capability

R. G. STRAUCH
W. C. CAMPBELL
R. B. CHADWICK
K. P. MORAN

BOULDER, COLO.
MAY 1975

U.S. DEPARTMENT OF COMMERCE
Rogers C. B. Morton, Secretary

NATIONAL OCEANIC AND ATMOSPHERIC ADMINISTRATION
Robert M. White, Administrator
ENVIRONMENTAL RESEARCH LABORATORIES
Wilmot N. Hess, Director

NOAA TECHNICAL REPORT ERL 329-WPL 39

FM-CW Boundary Layer Radar With Doppler Capability

R. G. STRAUCH
W. C. CAMPBELL
R. B. CHADWICK
K. P. MORAN

BOULDER, COLO.
May 1975

For sale by the Superintendent of Documents, U. S. Government Printing Office, Washington, D. C. 20402

CONTENTS

FIGURES

TABLE

FM-CW BOUNDARY LAYER RADAR WITH DOPPLER CAPABILITY

R. G. Strauch, W. C. Campbell,
R. B. Chadwick, and K. P. Moran

A high resolution FM-CW microwave boundary layer radar has been equipped with Doppler processing. The Doppler velocity spectrum is obtained from each range resolution cell by computing the power spectrum of the signal obtained from a sequence of consecutive sweeps. Target range is measured from the signal frequency by the usual FM-CW analysis techniques. Target velocity is obtained from a measurement of the signal phase in each sweep. The velocity spectrum of meteorological (distributed) targets can be measured whereas previously only the mean velocity of point targets could be obtained from this type of radar. Results obtained with snow tracers using a variety of sweep parameters demonstrate that the Doppler spectrum is easily obtained by a microwave FM-CW radar for altitudes below 2 km.

1. INTRODUCTION

This Technical Report describes the implementation and testing of full Doppler capability on an S-band FM-CW radar that is designed for boundary layer probing. "Full" Doppler capability means that the complete Doppler velocity spectrum is measured in each range resolution cell. The microwave FM-CW boundary layer probe was developed by Richter (1969) at the Naval Electronics Laboratory Center (NELC) for high resolution probing of the clear air boundary layer. A similar unit was built by Bean et al. (1971) at the Institute for Telecommunication Sciences. Another unit was completed at the Wave Propagation Laboratory (WPL) in May 1974. These radars have revealed clear air structures with a range resolution of less than 2 m. They are designed chiefly for zenith-pointing applications, although one of the radars built at NELC has limited scanning capability (Richter et al., 1973). The transmitter-receiver sections of the microwave FM-CW radars are similar, so the techniques described in this report could be used with other systems. Doppler capability has been added to the WPL radar.

2. PREVIOUS DOPPLER RESULTS

The mean velocity of a point target can readily be measured with an FM-CW radar by measuring the difference between the signal (mixer output) frequencies obtained during upsweep (transmitted frequency increasing with time) and downsweep (transmitted frequency decreasing with time). The signal frequency for upsweep is given by

$$f_u = \left| -\frac{2B}{cT} R - \frac{2V}{\lambda} \right| \tag{1}$$

and for downsweep by

$$f_d = \left| \frac{2B}{cT} R - \frac{2V}{\lambda} \right| \tag{2}$$

where B is the sweep width, T is the sweep time, R is the target range, c is the velocity of propagation, V is the radial velocity of the point target, and λ is the radar wavelength. The transmitted wavelength is not constant during the sweep, but the change in wavelength is assumed small compared with the wavelength at the start of the sweep. Comparison of upsweep and downsweep frequencies can be used to measure the velocity of isolated targets, but it cannot be used for distributed targets, such as raindrops, because the same signal frequency corresponds to scatterers at different locations in range-velocity space.

A second method of inferring target velocity is to measure the time rate of change of range. Since the boundary layer radar has a range resolution of about 1.5 m, the vertical velocity of insects or point echoes can readily be deduced by measuring the time required for the target to move between adjacent range cells. This techniques also enables one to estimate the radial velocity of a sharp edge of a meteorological target or any target with a distinctive feature. One of the problems is the length of time that the target must remain in the cone illuminated by the radar, particularly if the vertical velocity is small or precise velocity estimates are needed. The time required to measure the velocity spectrum with the techniques described in this report is comparable to the time required to measure the reflectivity.

Most radar meteorologists are interested in both the first moment (mean velocity) and second moment (velocity variance) of the Doppler velocity spectrum. The entire Doppler velocity spectrum may be of interest in some cases, particularly for a zenith-pointing radar. One of the limitations of the microwave boundary layer FM-CW radar has been its failure to provide Doppler data for the usual meteorological (distributed) target. Indeed, it has been widely believed that extracting the

Doppler spectrum from this type of radar was a formidable, if not impossible, task. However, Barrick (1973) has described a method by which the Doppler velocity spectrum has been obtained from FM-CW radars at lower (HF) frequencies. With this method, the Doppler spectrum of the backscatter from the sea surface was used to study the sea state with an FM-CW radar. The range may be hundreds of kilometers (time delays of milliseconds) for sea state radars. Consecutive sweeps must be phase coherent to obtain the Doppler spectrum. Phase coherent sweeps, where the transmitted phase is repetitive, can be generated at HF with frequency synthesizers. The signal return from N consecutive sweeps is processed to obtain the Doppler velocity spectrum.

The microwave boundary layer radars receive signals with time delays of a few microseconds but do not have phase coherent sweeps. The linear S-band sweep is generated with a YIG tuned transistor oscillator whose starting frequency (f_0), sweep width (B), and frequency or phase changes during the sweep will, in general, not be exactly the same for all N sweeps. However, because the range (time delay) is relatively short, the same processing scheme described by Barrick is applicable and the phase errors in the transmitted signal can be tolerated. We have implemented Doppler processing using the HF radar technique and tested it with no modifications to the microwave radar system; the Doppler capability was added by using a data acquisition and processing system developed for pulse Doppler radar to process the FM-CW signals.

3. THE FM-CW DOPPLER TECHNIQUE

The theory of processing FM-CW signals to obtain the Doppler spectrum will be briefly decribed in this section. The reader is referred to Barrick's work for a more complete discussion. The notation used here will be similar to Barrick's.

3.1 The Signal Phase

Let t = 0 denote the time at the start of the first sweep (fig. 1) and let T be the sweep time of a sawtooth sweep. N sweeps occur in NT seconds, referred to as "dwell time." Let t_i denote the time during any sweep. Then

$$t_i = t - nT \tag{3}$$

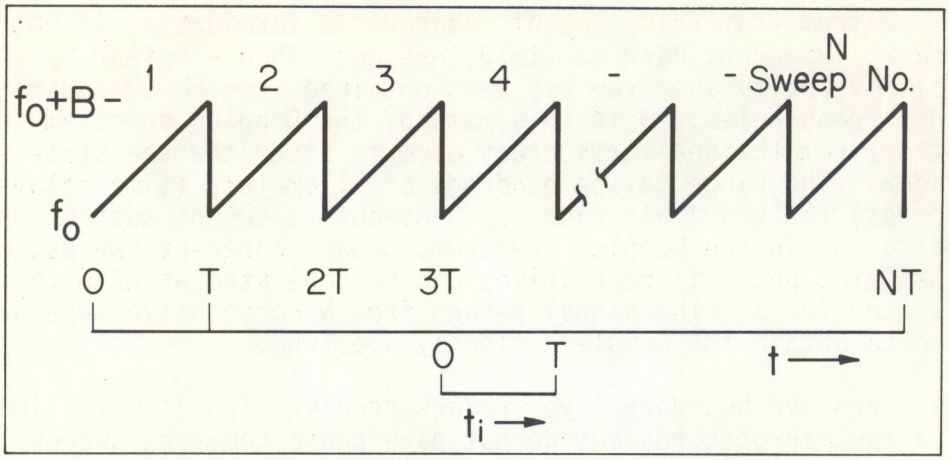

Figure 1. FM-CW sweep.

where n is the sweep index, $0 \leq n \leq N-1$, and $0 \leq t_i \leq T$. The signal obtained from a single scatterer can be written as

$$s(t_i) = A \cos [\phi (t_i)] \tag{4}$$

for $\tau \leq t_i \leq T - \tau$, where τ is the round trip time to the target,

$$\tau = \frac{2R}{c}, \tag{5}$$

and

$$\phi (t_i) = 2\pi [a t_i^2 + b t_i + c_0]. \tag{6}$$

The signal results from mixing the received microwave signal with the transmitted signal and discarding the sum terms from the output of the mixer. Although the transmitted signal lasts for T sec, the received signal lasts for $T - 2\tau$ sec because at the start of the sweep the microwave return corresponds to the previous sweep. Thus the mixed signal has a much higher frequency for τ sec at the start of the sweep. Likewise, at the end of the sweep the local oscillator (transmitter) is already starting the next sweep. τ will be a few microseconds and T

will be a few milliseconds, so the signal will have approximately T sec duration. The coefficients in the expression for the phase in (6) are given by

$$a = \frac{B\alpha}{T}\left(1 - \frac{\alpha}{2}\right), \tag{7}$$

$$b = f_0\,\alpha + B\left(\frac{\tau_0}{T} + n\alpha\right)(1 - \alpha), \tag{8}$$

and

$$c_0 = f_0\,\tau_0 + n\,f_0\,\alpha T - \frac{B\,\tau_0^2}{2T} - n\,B\,\alpha\left(\frac{n\,T\,\alpha}{2} + \tau_0\right), \tag{9}$$

where

$$\alpha = \frac{2V}{c} \tag{10}$$

and

$$\tau_0 = \frac{2\,R_0}{c}. \tag{11}$$

α is the normalized radial velocity; f_0 is the frequency of the start of the sweep; R_0 is the target range at $t = 0$. These expressions for a, b, and c_0 can be simplified by discarding all terms which, when multiplied by the maximum value of t_i, are much less than 1 so their phase contribution is negligible. The maximum value of t_i is T. Typical parameters that are used with the zenith-pointing S-band radar, enable us to simplify (6) to

$$\phi\,(t_i) = 2\pi\,(F\,t_i + \Phi) \tag{12}$$

where the frequency of the return signal is

$$F = \frac{B\,\tau_0}{T} + f_0\,\alpha + n\,B\,\alpha \tag{13}$$

and the phase of the return signal is

$$\Phi = f_0\tau_0 + nf_0\alpha T. \qquad (14)$$

The terms that must be retained for the zenith-pointing S-band radar at low altitudes are exactly the same terms retained by Barrick in his example using HF radar. Other terms must be retained if the range or transmitter frequency is increased so each set of sweep parameters must be examined to see which phase terms must be retained.

The three terms in the frequency, F, are:

1) The usual range term for an FM-CW radar, $B\tau_0/T$ or $2B\ R_0/cT$.

2) The Doppler shift, $f_0\alpha = 2V\ f_0/c = 2V/\lambda$, which is also contained in the usual FM-CW radar signal.

3) The accumulated range term, $nB\alpha$. This term arises because at the start of the n^{th} sweep, $t = nT$, the range has changed from R_0 to $R_0 + nTV$. Thus the range change is $nc\alpha T/2$ or $\Delta\tau = n\alpha T$. This change in time delay causes a frequency change of $B\Delta\tau/T = nB\alpha$.

The terms in the phase factor, Φ, are:

1) The elapsed phase, $f_0\tau_0$, which is the number of cycles of f_0 that occur during the time required for round trip propagation during the first sweep.

2) The accumulated phase, $nf_0\alpha T$. From above $nf_0\alpha T = f_0\Delta\tau$. $f_0\Delta\tau$ is the number of cycles of f_0 during the time required for round trip propagation for the accumulated range. This is the important term that leads to the Doppler spectrum.

The frequency, F, and the phase, Φ, change from sweep to sweep. The frequency change from sweep to sweep is $B\alpha$. If we restrict the velocity to that expected for vertical motion of meteorological targets, $nB\alpha$ may also be discarded. F is therefore approximately constant for the N sweeps. Conventional processing of FM-CW radar signals for the boundary layer radar ignores the Doppler term and determines the range by measuring F. The same technique will be used for Doppler processing; range will be determined (approximately) from F, but since the velocity will also be measured, the range can be corrected, if need be, because the Doppler term in F will be known.

The phase term, $nf_0\alpha T$, the only one that changes significantly from sweep to sweep, is the term that leads to the Doppler spectrum. The total phase term, Φ, also contains the constant $f_0\tau_0$. This constant term may be very large compared with $nf_0\alpha T$, so unless f_0 is sufficiently repetitive, changes in f_0 from sweep to sweep could mask the phase changes caused by target motion. The stability required is directly

proportional to τ_0 or target range. Thus the fact that the microwave FM-CW radar receives signals from the lowest 1 to 3 km of the atmosphere leads to tolerable stability requirements for the frequency at the start of the sweep.

3.2 Sampling the Signal

The Doppler measurement scheme relies on digital data processing techniques so the signal must be sampled and converted to digital words. M samples of the signal are taken during each sweep as shown in figure 2. The M samples are acquired during the time interval $T - 2\tau$ to eliminate the retrace effects discussed earlier. The samples are equally spaced in time and do not have to utilize the entire $T - 2\tau$ time slot available, but the sample gates must occur at the same time relative to the start of each sweep. The unused time in the sampling may be larger than that illustrated in figure 2. For example, in the implementation to be described in section 4, a triangular sweep was used and the entire downsweep portion was not sampled.

Sampling the signal during the sweep places an upper limit on the frequency, F.

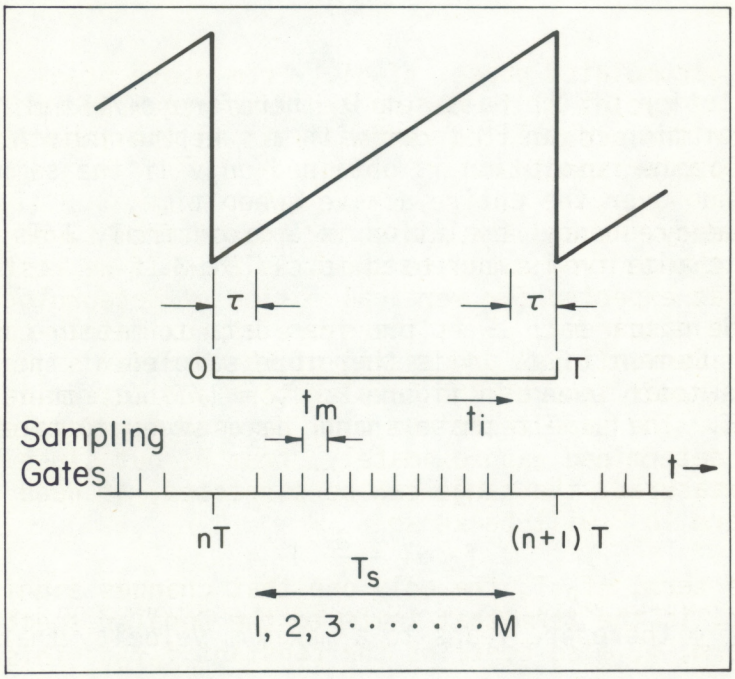

Figure 2. Timing for signal sampling.

If t_M is the time between samples, then the maximum signal frequency is

$$F_M = \frac{1}{2t_M} \tag{15}$$

and

$$t_M < \frac{T - 2\tau}{M - 1} \tag{16}$$

Normally M and t_M would be selected to extend the sampling interval over as much of the active sweep time as possible. The signal must be filtered prior to sampling to remove components with a frequency greater than F_M.

There are M samples acquired during each sweep so there will be M/2 resolution elements in the measurement of F and, as in conventional FM-CW radar signal processing, there will be M/2 range resolution cells. Sampling limits the maximum range interval that can be observed to

$$R_M = \frac{cT}{4Bt_M} \quad . \tag{17}$$

The range resolution of the data set is therefore $cT/2Bt_MM$. The available range resolution of an FM radar with a sweep bandwidth, B, is $\Delta R = c/2B$, but this range resolution is obtained only if the sampling interval, Ts, extends over the entire active sweep time, T. If Ts is less than T, then the frequency resolution is approximately 1/Ts or $1/Mt_M$ and the range resolution is increased to $cT/2Bt_MM$.

The signal return each sweep provides data to measure F and also provides a measurement of Φ. Φ is therefore sampled at the sweep rate, f_r. For the sawtooth sweep in figure 2, $f_r = 1/T$ but other sweeps may be used where $f_r < 1/T$. The phase change from sweep to sweep is given by

$$f_0 \alpha T = \frac{2V}{\lambda} T \quad .$$

The sampling of Φ therefore leads to a maximum velocity that can be measured since

$$\left| \frac{2V}{\lambda} T \right|$$

must be less than 1/2 to satisfy the Nyquist sampling theorem. Hence, for the sawtooth sweep the maximum velocity is given by

$$V_M = \pm \frac{\lambda}{4T} . \tag{18}$$

In general

$$V_M = \pm \frac{\lambda f_r}{4} . \tag{19}$$

This is the same relationship that applies to pulse Doppler radar. The N samples of Φ will provide N/2 velocity resolution elements so the velocity resolution is given by

$$\Delta V = \frac{\lambda f_r}{2N} . \tag{20}$$

3.3 Signal Processing

Barrick discusses two methods for processing the data samples. The first method involves a double Fourier transform, first computing the M/2-point complex transform of the M samples taken during each sweep, and then computing the N-point power spectrum of the N complex Fourier transform values associated with a fixed range gate or spectral index. The second method treats the M samples taken during all N sweeps as a single record of MN samples with a spacing of t_M. The power spectrum of this single long record gives the Doppler velocity spectrum for all the range gates. We used the second method to test the microwave FM-CW radar. A brief discussion of this method follows.

The power spectrum of the MN-point record is given by

$$P(f) \doteq \left[\frac{AT}{2}\right]^2 \left[\frac{\sin 2\pi (f - F) \frac{T}{2}}{\left(2\pi (f - F) \frac{T}{2}\right)}\right]^2 \left[\frac{\sin 2\pi\left(\frac{NT}{2}\right) (f - f_0 \alpha)}{\sin (2\pi)\left(\frac{T}{2}\right) (f - f_0 \alpha)}\right]^2 . \tag{21}$$

This expression was derived (essentially) by Barrick. The approximations used are those discussed earlier; F is assumed constant for the N sweeps and the signal from each sweep occurs for time T. No "windowing"

or weighting function is used. Fourier integrals are used to derive (21). The discrete transform of sampled signals gives samples of the power spectrum at

$$f = 0, 1/NT, 2/NT, \ldots . M/2T. \qquad (22)$$

The power spectrum will be a maximum at the spectral point where $f \doteq F$ and $f \doteq f_0 \alpha$. Note that $f_0 \alpha$ is the Doppler frequency, $2V/\lambda$. The $(\sin x/x)^2$term, which determines the range location of the target, is aperiodic with a main lobe whose full width between nulls is 2N spectral points. The half-power width of the main lobe is approximately N spectral points. The $(\sin Nx)^2/(\sin x)^2$ term, which determines the velocity of the target, is periodic with N spectral points. Its value is N^2 at $f = f_0 \alpha$, but is zero at $f = f_0 \alpha \pm 1/NT$, or one spectral point away from the maximum. Thus the $(\sin x)^2/(x)^2$ term establishes the range of the target by selecting N spectral points that could contain significant intensity while the $(\sin Nx)^2/(\sin x)^2$ term establishes the velocity by selecting one of these N points. All the power will be contained in a single spectral point if both F and $f_0 \alpha$ happen to equal a spectral index value. The sidelobes of the $(\sin x)^2/(x)^2$ and the $(\sin Nx)^2/(\sin x)^2$ functions show that, in general, the signal from a point target will also appear in sidelobes in the power spectrum. Weighting functions or window functions are used to reduce these sidelobes at the expense of a broadening of the main lobe.

The signal power returned by each scattering element is therefore resolved into its appropriate range-velocity location. The Doppler velocity spectrum for each range resolution cell is obtained from the data acquired during N sweeps.

3.4 Interpreting the Power Spectrum

The MN/2 points calculated from the MN-point signal record represent a two-dimensional range-velocity space. The discrete Fourier transform calculates a one-dimensional array that must be sorted into the proper range-velocity locations.

The zero velocity points are those spectral points where

$$\frac{\sin^2\left[2\pi\left(\frac{NT}{2}\right) f\right]}{\sin^2\left[2\pi\left(\frac{T}{2}\right) f\right]} = N^2 , \qquad (23)$$

or

$$f = 0,\ 1/T,\ 2/T,\ \ldots\ .\ M/2T \quad . \tag{24}$$

The zero velocity points are the "dc" point and every Nth spectral point since there are N spectral points in a 1/T interval. There are M/2 + 1 zero velocity points corresponding to M/2 + 1 range locations. The zero velocity points correspond to range locations

$$R = 0,\ \Delta R,\ 2\Delta R,\ \ldots\ .\ \frac{M}{2}\Delta R \tag{25}$$

since, at the spectral points given in (24),

$$F = \frac{2BR}{cT} = \frac{m}{T}$$

where m is the number of the range resolution cell and $0 \leq m \leq M/2$. The range resolution is c/2B because we have assumed the signal is available for T sec.

The spectral points corresponding to the maximum velocity can also be found from (21). At the maximum velocity, $f_0\ \alpha = 1/2T$ so the maximum velocity spectral points are

$$f = \frac{1}{2T},\ \frac{3}{2T},\ \frac{5}{2T},\ \ldots \tag{26}$$

The maximum velocity spectral points are associated with two adjacent range locations. That is, the spectral point for the positive maximum velocity for the m^{th} range location is also the negative maximum velocity point for the (m + 1) range location.

The Doppler shift for a receding target reduces the received microwave frequency, but the frequency of the mixer output increases because the "local oscillator" frequency is higher than the signal frequency. If the radial velocity is away from the radar, the range increases from sweep to sweep, the phase increases from sweep to sweep, and the Doppler frequency term increases the signal frequency. Target motion away from the radar will therefore correspond to spectral points with index values higher than the zero velocity points, and target motion toward the radar will correspond to lower index values. There will be N/2 spectral points corresponding to positive velocities and N/2 corresponding to negative velocities associated with each range gate or zero velocity spectral point. Note however that in the first range gate, corresponding to f = 0, the spectrum for index values less than zero is folded

onto the spectrum for positive index values. Thus there will be only N/2 velocity resolutions for the first range location and the sign of the velocity will not be resolved. A similar effect occurs in the last range location. There will be N/2 velocity resolution elements for the last range location because the spectrum is folded at the spectral point f = M/2T, the zero velocity spectral point of the last range location. Therefore, although there are M/2 + 1 range locations, the sign of the velocity is resolved in only M/2 - 1 range locations.

4. ADDITION OF DOPPLER PROCESSING TO A MICROWAVE FM-CW RADAR

The feasibility of obtaining Doppler spectra with the microwave FM-CW boundary layer radar was tested by recording and analyzing the FM signals with a data system developed for a pulsed Doppler radar. No changes were made to the FM-CW radar. The pulsed Doppler data system used two voltage outputs from the FM radar: the signal output from the mixer and the trigger that marks the start time for the upsweep. The FM radar has a triangular sweep with variable amplitude and sweep rates. The downsweep is not used for acquiring data. The pulse Doppler data system treated each FM sweep as a single radar pulse, i.e., we have a time delay after the trigger followed by the acquisition of M equally spaced samples. For pulse Doppler radar, the time delay is the range to the first range gate, and the spacing between samples is the range gate spacing. N sweeps were acquired to form a single record of 2048 samples. The pulse Doppler processor software instructions were modified to have the record analyzed as though it had been acquired from a single range gate of a pulsed radar with 2048 transmitted pulses. The output of the processor is a 1024 point power spectrum. The record length was fixed at 2048 samples so that existing software could process the data. Even with this limitation the versatility of the data system allows a selection of various range and velocity parameters.

4.1 Sweep and Sampling Characteristics

Various sweeps were selected to test the Doppler capability with a variety of range and velocity resolutions. The sweep rates were selected to establish unambiguous velocity intervals that could resolve the spectra of precipitation particles as well as the expected spectra of clear air returns. Thirty-two sweeps (velocity resolution elements) were used in each test, with 64 samples taken during each sweep (32 range locations). Bandwidths with convenient range resolutions were selected. The FM sweep is generated with a digital counter and a 16-bit

digital-to-analog converter. The sweep amplitude (B) is selected by setting the number of counts before changing direction. The count rate and count amplitude select the sweep rate (f_r). The sweep parameters that were tested are listed in Table 1. (The possible number of sweep parameters is about 10^5.) In all cases the maximum velocity times the dwell time was less than the range resolution. If this condition is not satisfied, the signal will appear in more than one range location but with reduced intensity. Also, the approximations needed to reduce the complete expressions for the frequency and phase to the approximate relationships given by (13) and (14) are applicable for all the test sweeps.

The spacing between samples, t_M, establishes the maximum frequency F_M which, in turn, determines the maximum range. There are two factors that must be considered in determing the range resolution—the available resolution from the radar, c/2B, and the resolution of the data set, $R_M/(M/2 + 1)$. These two values will be identical only if the M samples span the entire time of the active sweep. If the data samples do not cover the entire time (T) of the active sweep, the maximum frequency (and therefore maximum range) will be increased with no corresponding increase in the number of range locations. Hence, because the samples can not cover the entire active sweep time for reasons discussed previously, c/2B will always be less than $R_M/(M/2 + 1)$.

Note that the sampling interval, $(M - 1)\, t_M$, is considerable smaller than T or $T - 2\tau$ in all cases. Transients are introduced in the sweep circuit at the turn-around points in the sweep. A relatively long delay after turnaround allowed time for the sweep to settle. If a sawtooth sweep had been used, even more settling time would have been required or the start of the upsweep would have had to be delayed following retrace. Therefore the maximum sweep rate, and the resulting maximum unambiguous velocity, would be about the same for a sawtooth sweep as for a triangular sweep. The effect of using a triangular sweep, as opposed to a sawtooth sweep of the same sweep rate, is to double the dwell time and improve the velocity resolution by a factor of 2.

After the signal was filtered with a low pass filter having a cutoff frequency equal to 0.8 of the Nyquist frequency, it was sampled with an 8-bit analog-to-digital converter and recorded on magnetic tape.

4.2 Data Processing

We analyzed the 2048-point records with a NOVA-800 minicomputer using a fast Fourier transform algorithm to compute the discrete Fourier transform. The data samples were weighted with a Hanning weighting function applied to the long record. This weighting will reduce the velocity sidelobes. The M samples for each sweep should also be weighted as illustrated in figure 3 to reduce the range sidelobes. This second

Table 1. Sweep Parameters Tested for Doppler Capability.

V_M	f_r	T	T_D	ΔV	t_M	T_s	F_M	B	R_M	ΔR	D
Maximum Velocity	Sweep Rate	Upsweep Time	Dwell Time	Velocity Resolution	Sample Spacing	Sampling Interval	Maximum Signal Frequency	Sweep Width	Maximum Range	Radar Resolution	Range Resolution
m sec^{-1}	sec^{-1}	millisec	sec	m sec^{-1}	μsec	millisec	KHz	MHz	m	m	m
±1	40	12.5	0.8	1/16	128	8.06	3.91	16.66	443	9	13.4
								10.00	733	15	22.2
								7.14	1027	21	31
								5.55	1320	27	40
								4.54	1615	33	49
±2.5	100	5	0.32	5/32	64	4.03	7.82	20.0	293	7.5	8.9
								10.0	586	15	17.7
								5.0	1171	30	35.5
								3.33	1757	45	53.2
								2.50	2343	60	71
±5	200	2.5	0.16	5/16	30	1.89	16.6	10.0	622	15	18.8
								5.0	1245	30	37.7
								3.33	1868	45	56.6
								2.50	2490	60	75.5
								2.0	3114	75	94.4
±8	320	1.5625	0.1	1/2	17	1.07	29.5	6.50	1060	23	32
								3.12	2207	48	67
								2.08	3310	72	100
								1.56	4408	96	133
								1.25	5520	120	167

$V_M = \pm \frac{\lambda f_r}{4}$ $\quad \Delta V = \frac{2V_M}{N}$ $\quad T_s = (M - 1)\, t_M$ $\quad F_M = \frac{1}{2t_M}$ $\quad \Delta R = c/2B$

$\lambda \doteq 0.1$ m $\quad T_D = N/f_r$ $\quad M = 64$ $\quad R_M = \frac{cT\, F_M}{2B}$ $\quad D = \frac{R_M}{M/2 + 1}$

$T = \frac{1}{2f_r}$ $\quad N = 32$ $\quad f_0 = 2.9$ GHz

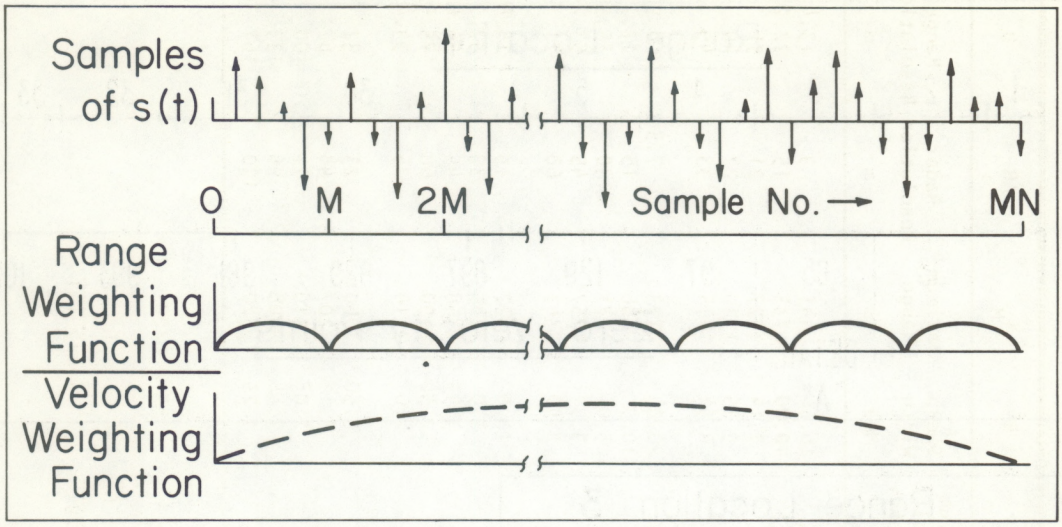

Figure 3. Weighting functions.

weighting was not used so the range sidelobes are relatively large. The 1024-point power spectrum is printed in order of increasing spectral index. The correspondence of range and velocity to the spectral index is shown in figure 4.

5. TEST RESULTS

Figure 5 illustrates the power densities measured with a delay line used to simulate a stationary target. The signal from the 2.5 μsec delay line appears at a range of 375 m and, because of reflections, also appears at 1125 m. The power density measured at the 33 zero-velocity spectral points is plotted in figure 5a (power density less than 0 dB is plotted as 0 dB in all the figures). Note that the range sidelobes cause the delay line to appear at more than one range location. The peak sidelobe level is typically 10 to 20 dB below the signal level in the correct range location. The results confirm the range resolution and maximum range calculated in Table 1.

The velocity spectrum for the range location that corresponds to the actual range for the delay line is shown in figure 5b. Note that although figure 5a shows the delay line signal in spectral locations that are ± 32, ± 64, etc., points removed from the spectral point corresponding to 375 m (and zero velocity), figure 5b shows there is no measurable power density only two spectral points away from the zero velocity point. The delay line target provides a convenient test target that insures the system is working as predicted.

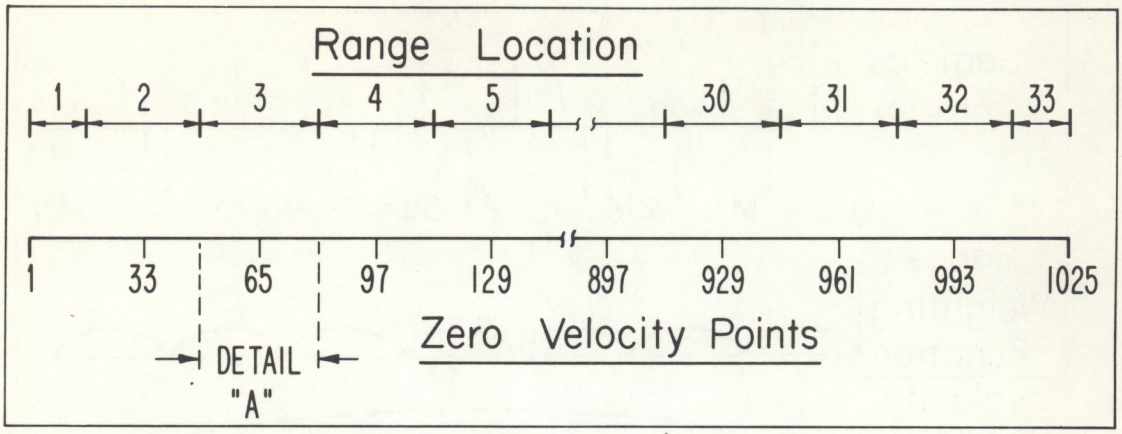

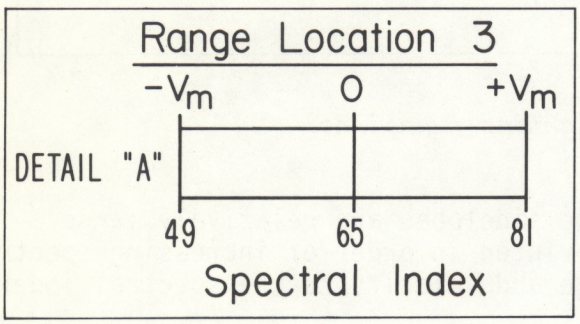

Figure 4. Range and velocity correspondence to the spectral index.

Figure 6 shows fall velocity spectra of snow, obtained with the FM radar at different maximum velocity settings. These spectra were verified by similar spectra obtained with the pulse Doppler radar. Notice the velocity folding that occurs when the preselected maximum velocity, V_m, is only $\pm$ 1 m sec^{-1} (fig. 6a). The four spectra in figure 6 were not measured at the same receiver gain. The signal occurs in fewer spectral locations as the maximum velocity is increased. The data in figure 6 were acquired without using the traveling wave tube (TWT) power amplifier. The TWT has a history of problems with noise and spurious modulation. The spectra of the delay line test target show increased noise when measured with the TWT output. Figure 7 illustrates results obtained in snow, with different range resolutions, using the TWT. The spectra for snow do not appear to be degraded by the TWT, but the delay line test is a more sensitive test for the noise caused by spurious modulation because the receiver noise is negligible for such an ideal target.

Deviations from the ideal and repetitive transmitted phase will degrade the velocity spectrum. Since the signal from the mixer is the phase difference between the transmitted phase at time t and t + τ, the

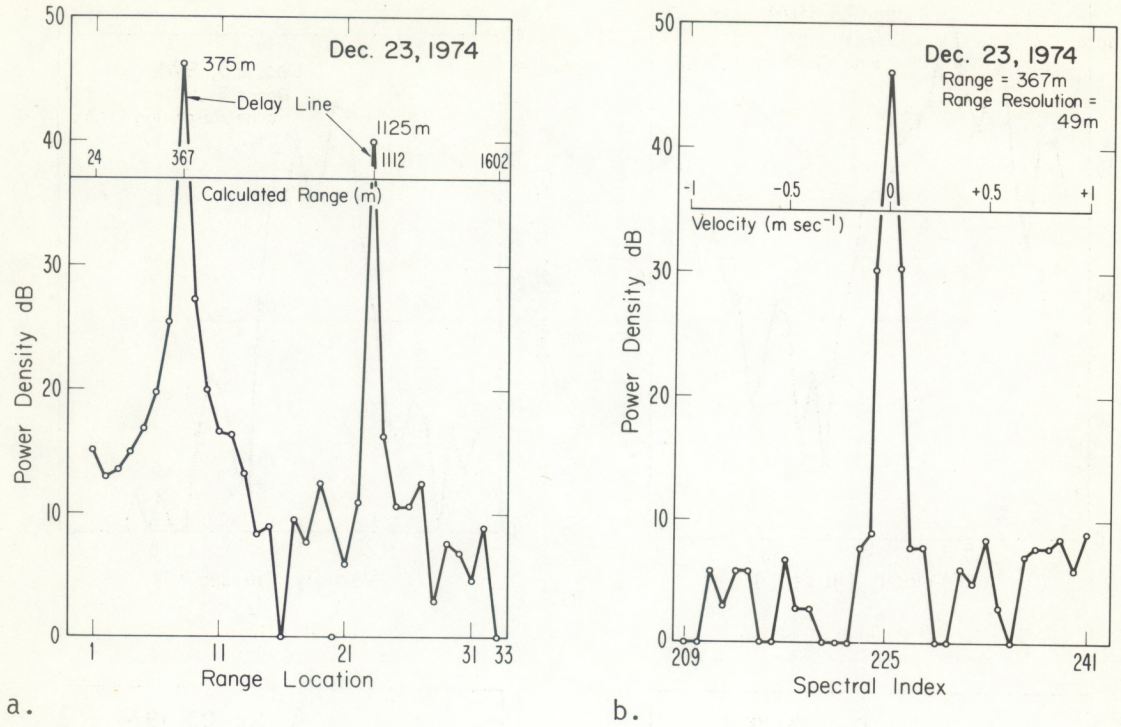

Figure 5. a. Power density at the zero-velocity spectral points; a 2.5 microsecond delay line was used to simulate a fixed target. b. Velocity spectrum of a 2.5 microsecond delay line.

phase errors will be first observed at long range. Consider the term $f_0\tau_0$ in the expression for Φ. This term is usually by far the largest term in the argument of $\phi(t_i)$. f_0 will vary from sweep to sweep because of long term drift and noise in the oscillator and because of drift and noise in the sweep circuits that control the frequency. Random fluctuations of $f_0\tau_0$ from sweep to sweep add a noise component to the signal phase that will reduce the signal-to-noise ratio in the spectrum. Rms fluctuations of f_0 of one part in 10^5 will cause rms phase fluctuations of 0.12 radians per 100 m range. If the instability of f_0 is this large, the velocity spectrum should be noticeably degraded at ranges greater than 1 km and probably not usable at more than 4 km range, because the phase of the Doppler signal would be masked by the random phase being added by the $f_0\tau_0$ term.

Figure 8 shows the spectrum of the delay line target at 1125 m. Receiver noise is negligible. There is almost no noise in the range locations where the delay line does not appear. The noise is therefore caused by nonideal signal phase. Figure 8 and figure 5b, from the same record, show there is a noticeable degradation in the signal-to-noise ratio for the delay line signal at 1125 m compared with the delay line

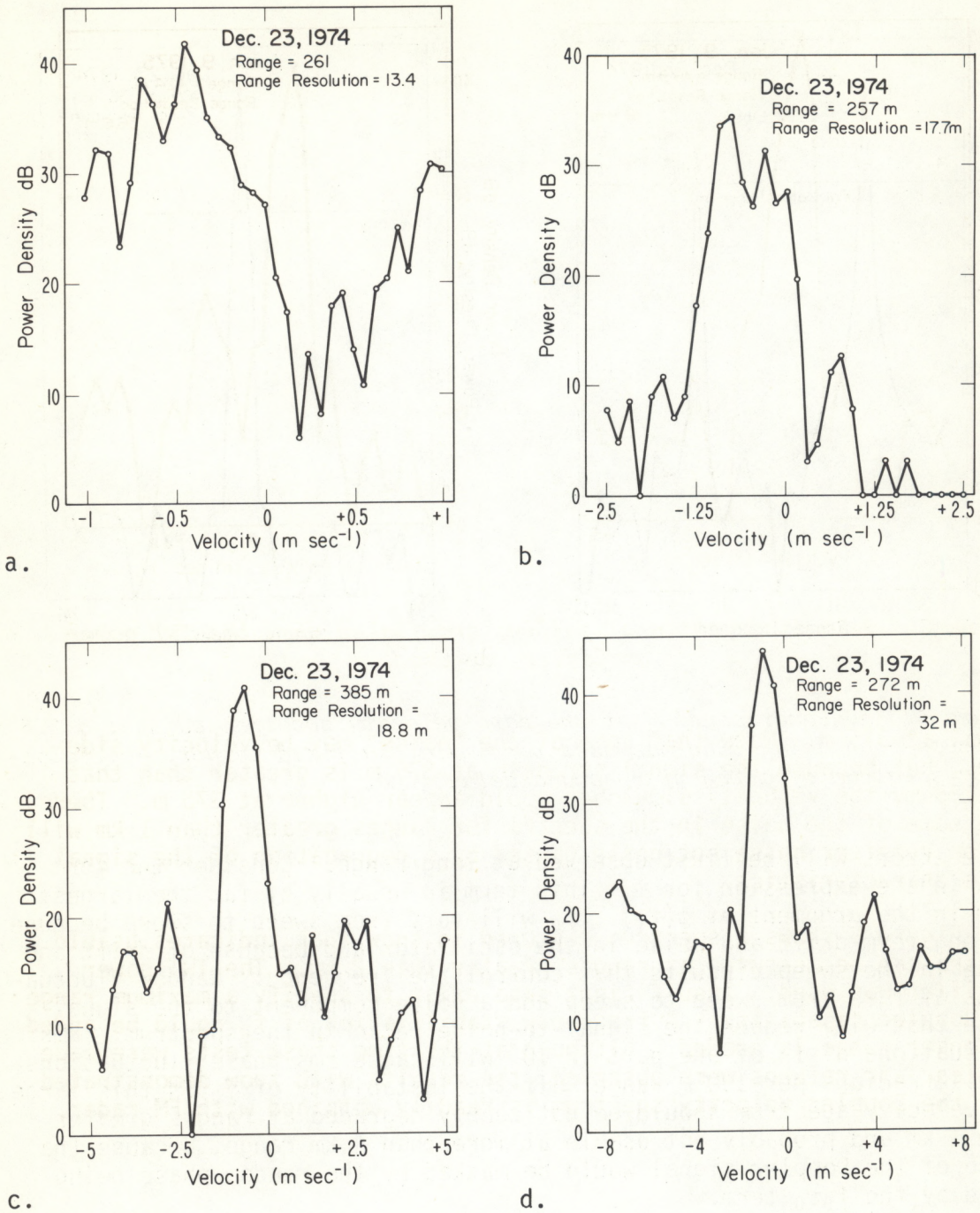

Figure 6. Velocity spectra of falling snowflakes observed at different maximum unambiguous velocities. a. ±1 m sec^{-1}; b. 2.5 m sec^{-1}; c. 5 m sec^{-1}; d. 8 m sec^{-1}.

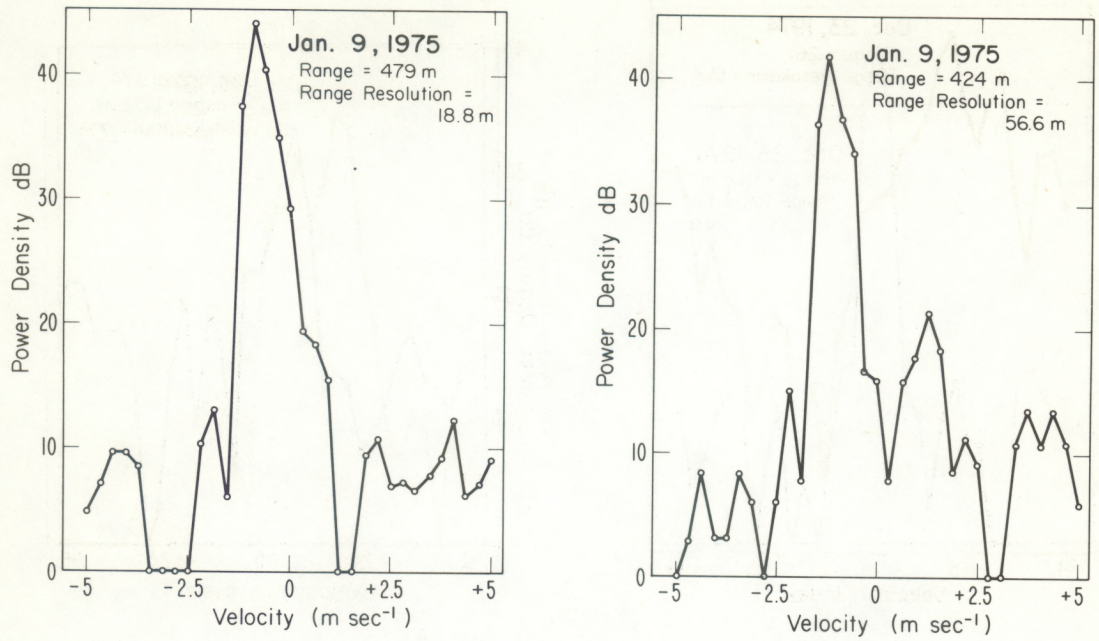

Figure 7. Velocity spectra of falling snowflakes when the TWT power amplifier was used.

signal at 375 m. Note that some of the "noise" may be velocity sidelobes, but because the signal strength at 375 m is greater than that at 1125 m, the velocity sidelobes would appear higher at 375 m. Therefore some of the noise in the spectra for ranges greater than 1 km will not be receiver noise but noise caused by a degradation of the signal phase characteristics.

Figure 9 shows a spectrum measured in snow that indicates usable spectra can be measured at ranges greater than 2 km. The TWT power amplifier was used. Insufficient data exist to specify a maximum range for Doppler capability. A frequency stabilization of f_0 could be added if longer range is needed. Although at the time these tests were made no clear air returns were observed, the results with snow demonstrated that the Doppler velocity spectrum is readily obtained with FM radar.

6. CONCLUSIONS

A recent report by McCormick and Tangerud (1974), referring to the microwave FM-CW boundary layer probe, states "The FM-CW radar has a serious disadvantage in addition to its high cost. That is, that it is inherently incapable of measuring the radial velocity of the target,

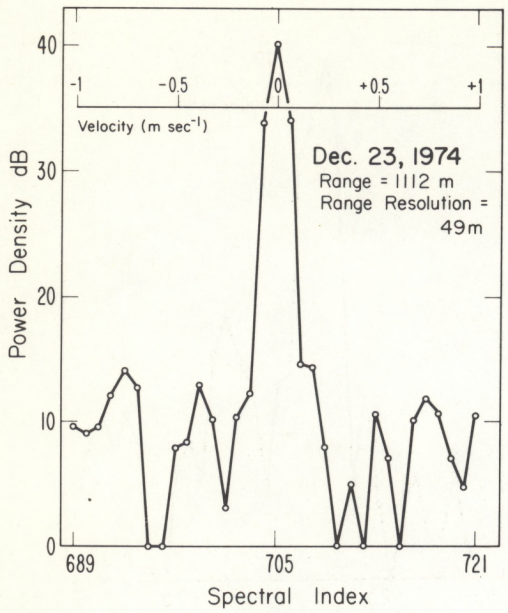

Figure 8. Velocity spectrum of 7.5 microsecond delay line target.

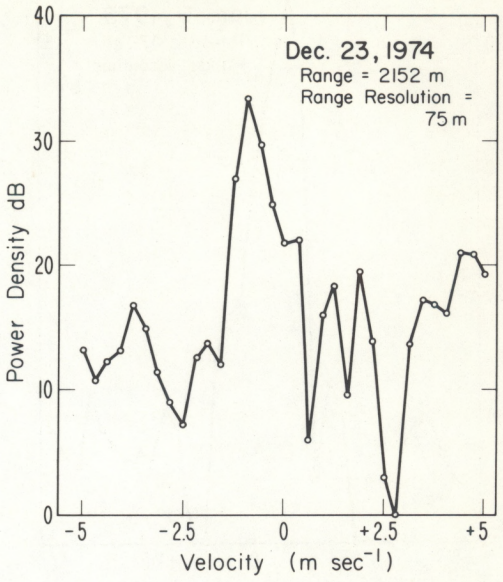

Figure 9. Velocity spectrum of falling snow at "long" range when TWT power amplifier was used.

since a radial velocity causes the signal to appear at a slightly incorrect range." It has been widely believed that obtaining the Doppler velocity with an FM radar, if not impossible, would be very difficult. The results obtained in tests described in this report show that the complete Doppler velocity spectrum for each range location is readily measured by the FM radar (at low range). The only hardware required to add Doppler capability for postanalysis is a recorder for the mixer output.

The tests described in this report did not utilize the fine scale range resolution of the FM-CW radar. The main reason for this was the restriction to 2048 total samples so the data could be processed with existing software. The results illustrated in this report show that a 32-point velocity spectrum is acceptable for at least some applications. A total record length of 8192 points would give the versatility needed to operate in precipitation or clear air with good range and velocity resolution. A record length of 8192 samples would give 128 range cells with 32-point velocity spectra or 64 range cells with 64-point velocity spectra. The data could be improved over that illustrated here by using both the range and velocity weighting functions. In addition, the reflectivity profiles measured with the FM radar can be improved with the

addition of Doppler processing because the ground return can be removed and the actual signal strength recovered, particularly in those cases where the velocity spectra do not extend through zero velocity.

The FM-CW boundary layer radar with Doppler capability has potential research application in both precipitation and clear air return. The superior range resolution makes possible the measurement of velocity and velocity variance profiles at scale sizes that are not observed by pulsed radars. Also, the FM-CW radar can measure the vertical velocity spectrum at such low altitudes that vertical air motion can be neglected. The Doppler velocity spectrum measured at very low altitudes can be converted to a drop size distribution.

In clear air return the vertical Doppler velocity is the vertical air motion. Measurement of the vertical air motion should add to the understanding of the clear air structures that are observed in the boundary layer. Perhaps even more important is the second moment of the velocity spectrum in clear air. The measured second moment can be used to estimate the turbulent dissipation rate. If the turbulence can be estimated the clear air radar measurements may lead to an improved quantitative description of the scattering mechanism.

7. REFERENCES

Barrick, D. E., 1973: FM-CW radar signals and digital processing, *NOAA Technical Report ERL 283-WPL-26.*

Bean, B. R., R. E. McGavin, R. B. Chadwick, and B. D. Warner, 1971: Preliminary results of utilizing the high resolution FM radar, *Boundary Layer Meteor., 1*, 466-473.

McCormick, K. S. and A. J. Tangerud, 1974: A lower power high resolution radar for tropospheric studies, *Norwegian Defence Research Establishment, FFIE, Teknisk Notat E-652.*

Richter, J. H., 1969: High resolution radar sounding, *Radio Sci., 4*, 1261-1268.

Richter, J. H., D. R. Jensen, R. A. Poppert, and V. R. Noonkester, 1973: New developments in FM-CW radar sounding, *Boundary Layer Meteor., 4*, 179-200.

☆ U.S. GOVERNMENT PRINTING OFFICE: 1973 — 677-242 / 1271 REGION NO. 8

ENVIRONMENTAL RESEARCH LABORATORIES

The mission of the Environmental Reasearch Laboratories is to study the oceans, inland waters, the lower and upper atmosphere, the space environment, and the earth, in search of the understanding needed to provide more useful services in improving man's prospects for survival as influenced by the physical environment. Laboratories contributing to these studies are:

Atlantic Oceanographic and Meteorological Laboratories (AOML): Geology and geophysics of ocean basins and borders, oceanic processes, sea-air interactions and remote sensing of ocean processes and characteristics (Miami, Florida).

Pacific Marine Environmental Laboratory (PMEL): Environmental processes with emphasis on monitoring and predicting the effects of man's activities on estuarine, coastal, and near-shore marine processes (Seattle, Washington).

Great Lakes Environmental Research Laboratory (GLERL): Physical, chemical, and biological, limnology, lake-air interactions, lake hydrology, lake level forecasting, and lake ice studies (Ann Arbor, Michigan).

Atmospheric Physics and Chemistry Laboratory (APCL): Processes of cloud and preciptation physics; chemical composition and nucleating substances in the lower atmosphere; and laboratory and field experiments toward developing feasible methods of weather modification.

Air Resources Laboratories (ARL): Diffusion, transport, and dissipation of atmospheric contaminants; development of methods for prediction and control of atmospheric pollution; geophysical monitoring for climatic change (Silver Spring, Maryland).

Geophysical Fluid Dynamics Laboratory (GFDL): Dynamics and physics of geophysical fluid systems; development of a theoretical basis, through mathematical modeling and computer simulation, for the behavior and properties of the atmosphere and the oceans (Princeton, New Jersey).

National Severe Storms Laboratory (NSSL): Tornadoes, squall lines, thunderstorms, and other severe local convective phenomena directed toward improved methods of prediction and detection (Norman, Oklahoma).

Space Environment Laboratory (SEL): Solar-terrestrial physics, service and technique development in the areas of environmental monitoring and forecasting.

Aeronomy Laboratory (AL): Theoretical, laboratory, rocket, and satellite studies of the physical and chemical processes controlling the ionosphere and exosphere of the earth and other planets, and of the dynamics of their interactions with high-altitude meteorology.

Wave Propagation Laboratory (WPL): Development of new methods for remote sensing of the geophysical environment with special emphasis on optical, microwave and acoustic sensing systems.

Marine EcoSystem Analysis Program Office (MESA): Plans and directs interdisciplinary analyses of the physical, chemical, geological, and biological characteristics of selected coastal regions to assess the potential effects of ocean dumping, municipal and industrial waste discharges, oil pollution, or other activity which may have environmental impact.

Weather Modification Program Office (WMPO): Plans and directs ERL weather modification research activities in precipitation enhancement and severe storms mitigation and operates ERL's research aircraft.

NATIONAL OCEANIC AND ATMOSPHERIC ADMINISTRATION
BOULDER, COLORADO 80302